The constant stress tensile creep behaviour of a superplastic zirconia–alumina composite

D. M. OWEN*, A. H. CHOKSHI‡
Department of Applied Mechanics and Engineering Sciences, University of California, San Diego, La Jolla, CA 92093, USA

A detailed study was conducted to evaluate the constant stress tensile creep behaviour of a superplastic 3 mol% yttria-stabilized zirconia–20 wt% alumina composite. The comprehensive experimental results indicate that creep deformation may be expressed in the form $\dot{\varepsilon} \propto \sigma^{2.8}(1/\bar{L})^2 \exp(-585\,000/8.3\,T)$, where $\dot{\varepsilon}$ is the steady-state creep rate, σ is the imposed stress, $\bar{L}$ is the linear intercept grain size and T is the absolute temperature. Microstructural observations revealed that there is very little dislocation activity, or change in grain size or shape. A detailed analysis was conducted to evaluate the possible rate-controlling mechanisms in terms of the experimentally determined mechanical properties and the microstructural observations. Based on the maintenance of an equiaxed microstructure and the strong grain size and stress dependence, it is concluded that creep occurs by a grain-boundary sliding/grain rearrangement process.

1. Introduction

Although the early studies on superplasticity were restricted largely to fine-grained metallic alloys [1–3], it is now recognized that large ductilities may also be obtained in intermetallic compounds and ceramics [4, 5]. The recent report by Wakai et al. [6] on superplasticity in a commercially viable yttria-stabilized zirconia has spurred considerable interest in superplastic ceramics, and superplasticity has been reported now in a wide range of ceramics [4, 5]. In contrast to metallic alloys, there is little detailed information available on the creep characteristics of superplastic ceramic composites.

The elevated temperature mechanical properties of superplastic materials may be represented as

$$\dot{\varepsilon} = \frac{ADGb}{kT}\left(\frac{b}{d}\right)^p\left(\frac{\sigma}{G}\right)^n \qquad (1)$$

where $\dot{\varepsilon}$ is the steady-state strain rate, D is the diffusion coefficient, G is the shear modulus, b is the magnitude of the Burgers vector, k is Boltzmann's constant, T is the absolute temperature, σ is the imposed stress, d is the grain size, and A, p and n are constants. The diffusion coefficient may be expressed as $D = D_0 \exp(-Q/RT)$, where D_0 is a frequency factor, Q is the activation energy for the rate-controlling process and R is the gas constant. A low stress exponent, n, promotes stable tensile deformation, and superplasticity is usually associated with values of $n < 3$.

An examination of the available data on superplastic ceramics reveals that contradictory data are reported frequently for the mechanical characteristics of nominally identical materials. Three specific factors relevant to the present investigation are considered

below: (i) stress exponent, (ii) transitions in deformation mechanism, and (iii) deformation parameters and mechanisms.

The stress exponent for superplastic deformation in ceramics has not yet been identified unambiguously. Thus, for example, Wakai et al. [6] and Nieh et al. [7] reported stress exponents of ~ 2 and 3, respectively, for the superplastic deformation of a 3 mol% Y_2O_3 stabilized tetragonal zirconia obtained from the same source. Carry [8] has attributed these differences to variations in trace levels of impurities, which may influence the formation of amorphous glassy layers along grain boundaries. However, Yoshizawa and Sakuma [9] demonstrated that the stress exponent was not affected significantly by deliberate additions of commercial glasses to a superplastic zirconia. In the investigations by Wakai et al. [6] and Nieh et al. [7], tensile specimens were tested in the as-received condition; extensive grain growth at elevated temperatures led to a substantial increase in flow stress during superplastic deformation [7]. It is possible that the reported differences in n values arise from microstructural instability, and the different procedures used in analysing experimental results.

Most studies on superplastic ceramics have been conducted under constant strain-rate conditions, over a rather limited range of strain rates of $\sim 10^{-4}$–10^{-2} s^{-1}. It is not clear whether, like metallic alloys, ceramics exhibit a transition from a superplastic to a non-superplastic region at lower strain rates. There is very little information on superplastic ceramics available at strain rates of $< 10^{-5}$ s^{-1}, and transitions in deformation mechanisms have not been examined in much detail. The limited data available

are inconsistent: thus, for example, Okamoto et al. [10] reported a decrease in stress exponent with a decrease in strain rate in a superplastic zirconia, whereas the data published by Nauer and Carry [11] suggest that there is an increase in stress exponent with a decrease in the strain rate in a ZrO_2. The identification of a rate-controlling mechanism is accomplished usually by comparing the experimental and theoretical values of n, p and Q. In view of the limited range of experimental conditions used in most investigations, and the often contradictory data reported, it has not been possible to identify unambiguously the rate-controlling deformation parameters and mechanism. Superplasticity in ceramics has been attributed variously to grain-boundary sliding [6], dislocation creep [7], diffusion creep [10], and interface-reaction-controlled diffusion creep [12].

The present investigation was undertaken to characterize in detail the mechanical properties of a superplastic ZrO_2-Al_2O_3 composite with the specific objectives of (i) identifying unambiguously the stress exponent, especially at lower strain rates, and (ii) evaluating critically the possible rate-controlling deformation mechanisms in light of the detailed characterization of the creep parameters and the microstructure.

2. Experimental procedure

The material chosen for this study was a 3 mol % Y_2O_3 stabilized ZrO_2-20 wt % Al_2O_3 composite. Flat tensile specimens with a gauge length of 12.7 mm were obtained from the Tosoh Corporation and the Nikkato Company in Japan. Both batches had an identical initial microstructure, and they exhibited identical static grain growth and creep characteristics; consequently, no distinction is made in this report between the data obtained from the two batches. The following chemical analysis was provided by the Nikkato Co. (wt %): Y_2O_3 = 3.92, Al_2O_3 = 19.53, SiO_2 = 0.002, Fe_2O_3 = 0.003, Na_2O = 0.014 and ZrO_2 = balance.

Tensile specimens were tested in a creep machine which utilized a specially designed cam to maintain a constant stress [13]. The flat tensile specimens were pin loaded to SiC pull rods, which were connected to universal joints to maintain specimen alignment. The creep strain was monitored continuously using a linear variable capacitance transducer connected either to the specimen loading pins and an alumina-rods extensometer or to the creep frame to measure the displacement of the pull rod: both techniques yielded very similar results. The signals from the capacitance transducer and a load cell were acquired, stored and displayed continuously on a personal computer. The tests were conducted in air and the temperatures were maintained to within ± 2 K of the desired values.

Constant stresses in the range of ∼ 4–100 MPa and temperatures in the range of ∼ 1600–1750 K were utilized in this investigation. A minimum of 10% engineering strain was recorded before the termination of any test. At a fixed temperature, specimens were tested either at a single stress or by using the stress change technique. Additional experiments were conducted by cycling the temperature at a fixed stress.

A coupon of the as-received material was polished and thermally etched by exposure to 1773 K for 1 h and examined by scanning electron microscopy (SEM). Prior to creep testing, the specimens were annealed in air at temperatures ranging from 1823–1923 K for up to 30 h to obtain a range of grain sizes. The grain sizes were measured from scanning electron micrographs and an image analysis system connected to a personal computer. The mean linear intercept phase sizes were measured in two orthogonal directions, $\bar{L}_1$ and $\bar{L}_2$, and the average phase size was defined as $\bar{L} = [\bar{L}_1 \bar{L}_2^2]^{1/3}$. The subscripts z and a are used in this report to identify the zirconia and alumina phases, respectively.

Selected specimens were examined by SEM after creep deformation to characterize changes in the microstructure such as grain growth and grain shape; these changes were evaluated both within gauge sections as well as in the grip sections, to isolate the effect of deformation. A limited number of specimens was also examined by transmission electron microscopy (TEM). Standard 3 mm diameter discs were ultrasonically drilled, ground to ∼ 100 μm thickness, dimpled and subject to ion-beam milling to produce electron-transparent specimens.

3. Results

In the as-received condition, the material exhibited an equiaxed microstructure with both the zirconia and alumina phases having a grain size $\bar{L}_z = \bar{L}_a = 0.4$ μm. Most of the experiments described in this report were conducted with specimens annealed for 10 h at 1823 K to produce a grain size of $\bar{L}_z = \bar{L}_a = 0.7$ μm. Fig. 1 is a scanning electron micrograph of a specimen annealed for 10 h at 1823 K, illustrating the equiaxed nature of the zirconia (light) and alumina (dark) phases. Annealing specimens at 1873 K for 30 h led to phase sizes of $\bar{L}_z = 1.5$ μm and $\bar{L}_a = 1.1$ μm, whereas annealing at 1923 K for 30 h led to phase sizes of $\bar{L}_z = 2.1$ μm and $\bar{L}_a = 1.5$ μm.

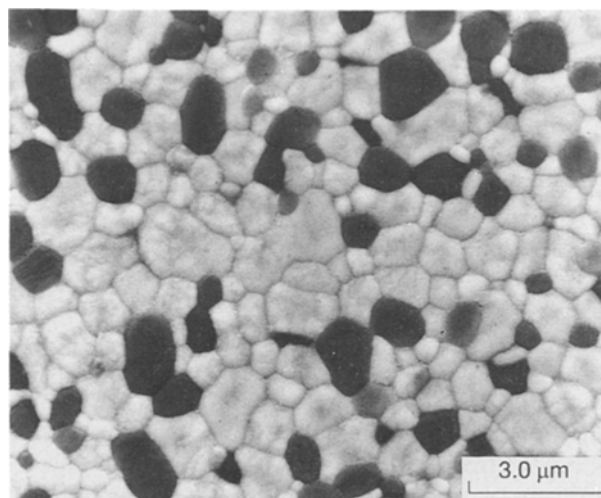The stresses remained constant to within 3% for all tests and true strain rates ranging from

Figure 1 Scanning electron micrograph of the zirconia-20% alumina composite with a grain size of 0.7 μm.

$\sim 10^{-8}$–10^{-3} s^{-1}. The gauge section deformed uniformly and there was some deformation in the pin loading area. The four specimens tested at the highest stress of 96 MPa fractured at elongations of $< 50\%$; all other experiments were terminated prior to failure. The machine used in this study was capable of maintaining a constant stress up to an elongation of 100%: a few specimens were tested to this limit.

3.1. Variation in strain rate with strain

The shapes of the tensile creep curves for some specimens tested at 1665 K are shown in Fig. 2 in the form of the variation in true strain rate with true strain. Inspection of these data indicates clearly that there is an extensive primary creep region extending to strains of $\sim 10\%$, over which the strain rate is decreasing significantly, and this is followed by a reasonably well-defined steady state. The longest experiment in the present investigation, at $\sigma = 4.5$ MPa, was terminated after a period of about 20 days. In the primary region, the level of change in strain rate with strain appears to increase with a decrease in the imposed stress. Inspection of the data from stress change experiments indicated that there was a very small transient following a stress change.

3.2. Dependence of strain rate on stress

The variation in steady-state creep rate with imposed stress is illustrated in Fig. 3 for specimens tested at 1665 K, either at a single stress (open datum points) or in a stress change experiment (filled datum points). The data for the stress change experiments correspond to strain rates at large strains. Clearly, there is very good agreement between data obtained from single stress and stress change experiments. All of the experimental data fall on a straight line with a correspond-

ing stress exponent of $n = 2.8 \pm 0.2$. Inspection of the results in Fig. 3 indicates that there is no change in stress exponent over the strain-rate range from $\sim 10^{-8}$–10^{-4} s^{-1}.

3.3. Influence of temperature on creep rate

The influence of temperature on creep rate was evaluated by conducting experiments on specimens with a grain size of $\bar{L}_z = \bar{L}_a = 0.7\,\mu$m at temperatures of 1598, 1665 and 1748 K, and constant stresses of either 21 or 96 MPa. The shapes of the creep curves were very similar over the temperature range used in this study. The apparent activation energy, Q_{app}, was determined from an Arrhenius plot of the steady-state strain rates versus reciprocal temperature, as shown in Fig. 4. The results indicate that an increase in temperature of 150 K leads to an increase in strain rate by almost two orders of magnitude. The values of Q_{app} were calculated to be 550 ± 25 and 570 ± 10 kJ mol^{-1} for stresses of 21 and 96 MPa, respectively. An activation energy of 640 ± 10 kJ mol^{-1} was obtained from a temperature cycling experiment.

3.4. Effect of grain size on creep rate

Experiments to evaluate the inverse grain size exponent, p, were conducted at $T = 1598$ K and stresses of either 21 or 96 MPa, using specimens with three different grain sizes. The shapes of the creep curves were not significantly affected by a change in grain size. It is clear from Equation 1 that the inverse grain-size exponent may be evaluated by plotting the data logarithmically as $\dot{\varepsilon}$ versus $\bar{L}$, at a constant stress. In microduplex structures, such as those in the composite used in this investigation, the grain size may be defined
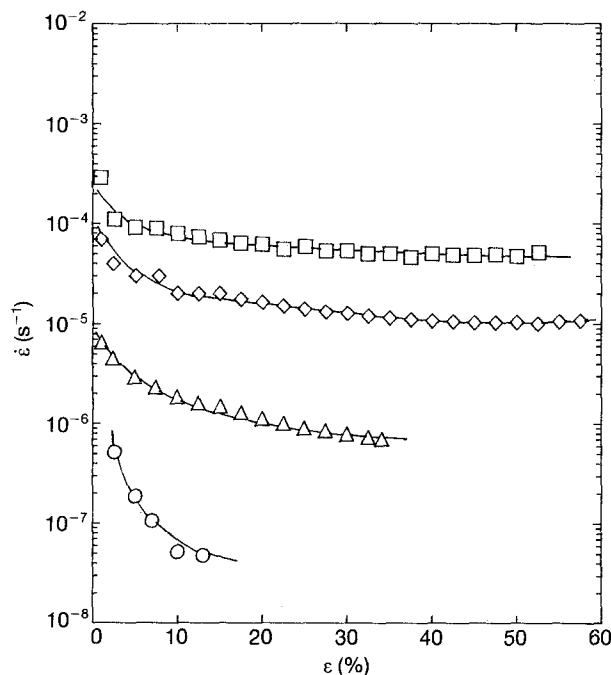

Figure 2 Variation in strain rate with strain for the ZrO$_2$–20% Al$_2$O$_3$ composite tested at 1665 K. $\bar{L}_z = \bar{L}_a = 0.7\,\mu$m. σ (MPa): ($\square$) 60, ($\diamond$) 30, ($\triangle$) 14, ($\bigcirc$) 4.5.
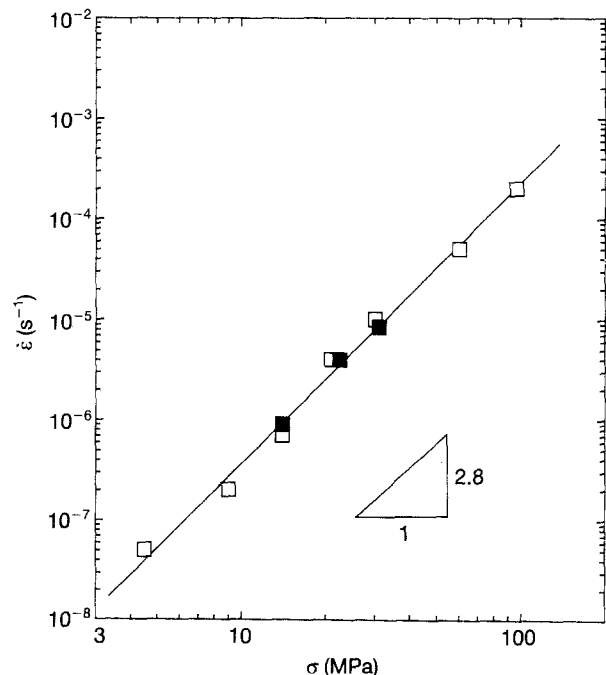
Figure 3 Variation in steady-state creep rate with stress for the composite tested at 1665 K. $\bar{L}_z = \bar{L}_a = 0.7\,\mu$m. ($\square$) single σ, ($\blacksquare$) σ change.
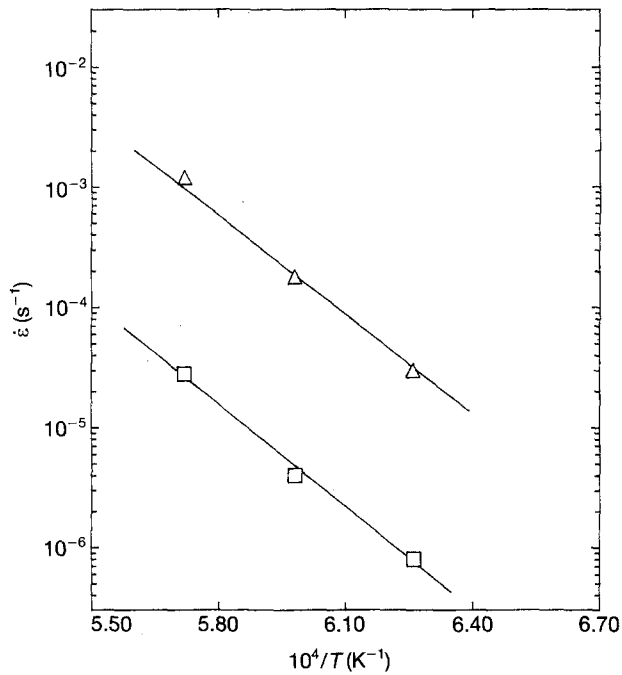
Figure 4 Arrhenius plot of the variation in strain with inverse temperature for the ZrO_2–20% Al_2O_3 composite. ($\triangle$) $\sigma = 96$ MPa, $Q_{app} = 570 \pm 10$ kJ mol^{-1}; ($\square$) $\sigma = 21$ MPa, $Q_{app} = 550 \pm 25$ kJ mol^{-1}.
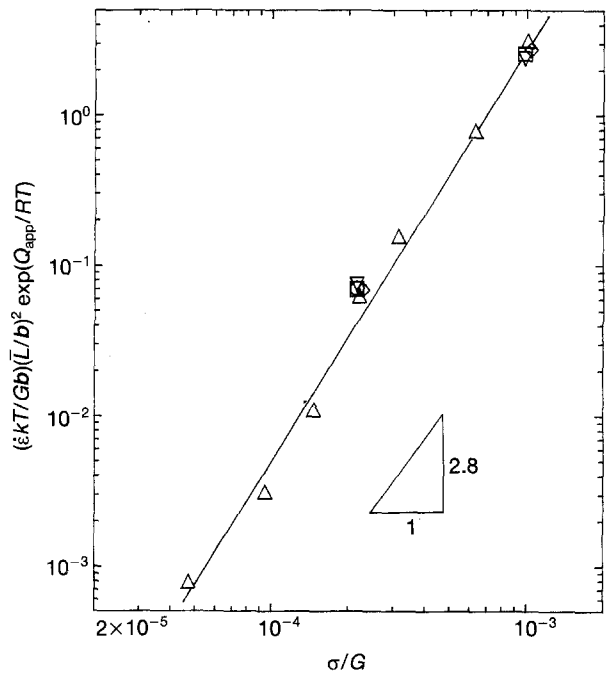

Figure 6 Variation in the temperature and grain-size compensated strain rate with the stress normalized by the shear modulus. T (k): ($\square$, ∇, $\bigcirc$) 1598, ($\triangle$) 1665, ($\diamond$) 1748. $\bar{L}_z$ (μm): ($\square$) 0.7, (∇) 1.3, ($\bigcirc$) 2.1, ($\triangle$, $\diamond$) 0.7.

3.5. The rate-controlling creep parameters

The present experimental study leads to the following rate-controlling creep parameters: $n = 2.8$, $p = 2$ and $Q = 585$ kJ mol^{-1}, which is average of the single temperature and temperature cycling values. It is clear from Equation 1, that it is possible to superimpose data from experiments conducted over a range of grain sizes and temperatures by suitably normalizing the creep results. Fig. 6 illustrates the variation in creep rate, normalized by the grain size and activation energy, with the flow stress normalized by the shear modulus. The variation in shear modulus with temperature was accounted for using data presented elsewhere [14, 15] and the shear modulus for the composite was taken to the volume average of the values for alumina and zirconia. Inspection of Fig. 6 indicates clearly that data from all of the present creep experiments superimpose reasonably on a straight line with a slope of 2.8. Based on these results, the constitutive equation for creep in the composite may be expressed as

$$\dot{\varepsilon} = (3.3 \pm 0.08) \times 10^8 \, (Gb/kT)(b/\bar{L})^{2.0 \pm 0.1}$$
$$\times (\sigma/G)^{2.8 \pm 0.2} \exp[(-585 \pm 45)/RT] \quad (2)$$

where $\dot{\varepsilon}$, G, b, k, L, σ and R have units of s^{-1}, Pa, m, J K^{-1}, m, Pa and J mol^{-1} K^{-1}, respectively.
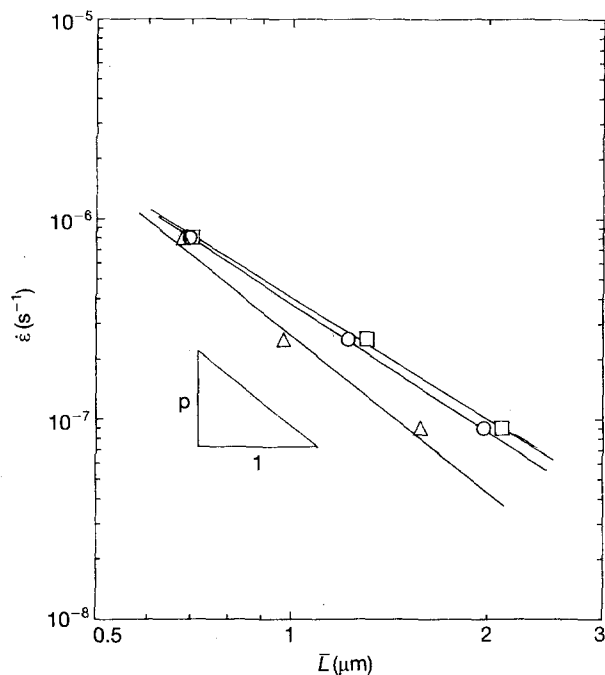

Figure 5 Variation in steady-state strain rate with grain size for the composite tested at 1665 K: the grain size may be defined in terms of the zirconia or alumina phases or their volume average. $\sigma = 21$ MPa. p: ($\square$) ZrO_2, 2.0 ± 0.1; ($\triangle$) Al_2O_3, 2.6 ± 0.6; ($\bigcirc$) Av. 2.1 ± 0.1.

in terms of (i) the phase size of zirconia, (ii) the phase size of alumina, or (iii) the volume average of the two phases. Fig. 5 illustrates the variation in strain with the average linear intercept length of the zirconia, alumina and volume average of the two phases, with corresponding values of p equal to 2.0 ± 0.1, 2.6 ± 0.6 and 2.1 ± 0.1, for specimens tested at a stress of 21 MPa. Based on $\bar{L}_z$, additional experiments at 96 MPa revealed that $p = 2$.

3.6. Microstructural changes accompanying creep deformation

Changes in phase sizes and aspects ratios were determined for selected specimens tested at 1665 K with an initial phase size $\bar{L}_z = \bar{L}_a = 0.7$ μm. The final average linear intercept sizes of the zirconia phase in the gauge section ranged from 0.67–0.84 μm, and from 0.64–0.78 μm in the gauge section for the alumina

phase. A comparison of the data in the gauge and grip sections indicated that, over the limited strains encountered in this study, deformation did not lead to a significant acceleration in the kinetics of grain growth. Noting that the initial phase sizes were $\bar{L}_z = \bar{L}_a$ $= 0.70$ μm, it is clear that there was very limited grain growth under the present experimental conditions. In addition, calculations indicate that there was very little increase in the aspect ratios of the two phases following superplastic deformation: the maximum values of the ratio $\bar{L}_1/\bar{L}_2$ were 1.35 and 1.16 for the alumina and zirconia phases, respectively.

Limited studies of the deformed specimens by transmission electron microscopy did not reveal any significant intragranular dislocation activity. X-ray diffraction analysis of the grip and gauge section indicated that there was no significant difference in the level of the monoclinic and tetragonal phases, although there appeared to be an increase in the level of monoclinic phase with increased exposure time at elevated temperatures.

4. Discussion

In spite of the many reports on superplasticity in zirconia and zirconia–alumina composites [16], there have been very few detailed studies in which the parameters controlling creep deformation have been identified unambiguously. One of the limitations of many investigations is that there was considerable grain growth during elevated temperature deformation, which made it difficult to characterize the mechanical properties. In addition, the possible differences in the sizes of the alumina and zirconia phases have not been noted. Also, the limited number of creep studies on superplastic ceramics have generally involved fairly low strains and, as noted elsewhere [17], these procedures may lead to erroneous evaluations of the stress exponent.

The following discussion focuses on an evaluation of the creep parameters and a critical examination of the possible rate-controlling creep mechanisms.

4.1. Evaluation of creep parameters
4.1.1. Stress dependence of creep deformation
The variation in steady state creep rate with stress, shown in Fig. 3, indicates that the data from single stress and stress change experiments can be represented reasonably with a stress exponent of $n \sim 2.8$. The strain rates from the single stress experiments at 1665 K at constant true strains of 5%, 10%, 20% and 30% yielded stress exponents of 2.4, 2.7, 2.8 and 2.8, respectively, thereby indicating that true strains of $> 10\%$ are necessary to characterize the steady-state creep behaviour of this composite. Clearly, the lack of attainment of steady-state deformation may lead to an inaccurate estimation of the stress exponent [17].

It is well known from experimental data on superplastic metallic alloys that spurious values of stress exponents may be obtained due to concurrent grain growth during superplastic deformation. The present

experimental results were obtained in the absence of significant grain growth, and they reveal that $n \sim 2.8$.

The present experimental data are in contrast with many of the previous studies on the ZrO_2–20 wt % Al_2O_3 composite material which reported $n \sim 2$ [18–21]. However, most of the earlier studies were limited to strain rates of $> 10^{-4} s^{-1}$ [18, 20, 21], whereas the present experimental creep study was conducted primarily at strain rates of $< 10^{-4} s^{-1}$. An early study on creep in the composite [19] may not be completely reliable due to the apparently small strains at which deformation was characterized, and the apparent lack of appropriate consideration for the presence of a significant primary creep region [17].

The above differences in the reported stress exponents may imply that there is a change in the stress exponent at a strain rate of $\sim 10^{-4} s^{-1}$, so that $n \sim 3$ at lower strain rates and $n \sim 2$ at higher strain rates. Such a transition was recently noted unambiguously in the compressive creep deformation of a 3 mol % yttria-stabilized zirconia [16, 22]. However, owing to the experimental limitations of the tensile creep apparatus, it was not possible to explore this possibility in the composite material.

4.1.2. Influence of grain size on creep
As illustrated in Fig. 5, substantially different values of p may be reported based on the definition of the grain size. In the present experimental study, the alumina phase is expected to be more creep resistant than the zirconia phase [23, 24]; in addition, zirconia is the major phase. Consequently, it is suggested that the zirconia phase size or a volume average phase size is an appropriate definition of the grain size for the composite material. Based on this discussion, the data in Fig. 5 indicate that $p \sim 2$ for the composite, independent of the imposed stress.

Nieh and Wadsworth [21] examined the influence of grain size on deformation in the composite. Using constant strain-rate experiments, they reported $\sigma \propto d^{0.75}$ [21]; these results, together with the reported value of $n \sim 1.5$, indicated a value of $p \sim 1.1$. (see Equation 1). However, it is important to note that there was significant grain growth in the earlier study, although the data reported were apparently corrected for grain growth.

4.1.3. Influence of temperature on creep
The present study yielded an apparent activation energy for creep equal to ~ 560 and $640 \, kJ \, mol^{-1}$ from experiments conducted at a constant temperature and by temperature cycling, respectively. This compares favourably with the activation energy of $\sim 620 \, kJ \, mol^{-1}$ for compressive superplastic deformation reported by Wakai et al. [18] and a value of $\sim 600 \, kJ \, mol^{-1}$ reported by Wakai and Kato [19] for tensile superplastic deformation in the composite material. However, it is substantially higher than the value of $\sim 260 \, kJ \, mol^{-1}$ reported by Nieh and Wadsworth [25]. There was significantly greater grain growth at the higher test temperatures utilized by

Nieh and Wadsworth [25], although the data used in calculating the activation energy were apparently corrected for grain growth.

It is interesting to note that the activation energy of ~ 550–600 kJ mol^{-1} obtained for deformation in the composite is very similar to that reported for superplastic deformation in the 3 mol % yttria-stablized zirconia [16] and to those for creep deformation in polycrystalline alumina [26]. It should be noted that there have been no direct tracer diffusion measurements of activation energies in tetragonal zirconia, and the available data on cubic zirconia are substantially less than the 500–600 kJ mol^{-1} range obtained in the composite. However, it is interesting to note that, over a larger temperature range, a combination of data from tracer diffusion, dislocation loop shrinkage and creep in cubic zirconia yielded an activation energy of ~ 490 kJ mol^{-1} [27, 28]. Such an activation energy is related to lattice diffusion in cubic zirconia, but it is not clear whether such data are relevant for deformation in a material predominantly containing the tetragonal zirconia phase.

4.1.4. Microstructural changes during creep

Prior to creep deformation, most of the specimens had phase sizes of $\bar{L}_z = \bar{L}_a = 0.70$ μm, and measurements indicated that there was very little grain growth during creep deformation. Thus, for example, the maximum zirconia and alumina phase sizes after creep deformation were recorded to be 0.82 and 0.78 μm after creep deformation at 4.5 MPa, which was the lowest stress and the longest-term experiment in this study. The somewhat lower grain growth observed in the alumina phase is consistent with the earlier report by Wakai and Kato [19] and Nieh et al. [29]. At the low strains used in this study, no significant differences could be detected in the grain sizes in the gauge and grip sections. At the larger strain utilized in other investigations [19, 29, 30], there was clear evidence for deformation-enhanced concurrent grain growth.

Careful measurements performed to determine changes in the grain shape indicated that there was very little tendency for grain elongation along the tensile axis: the alumina phase appeared to be slightly more elongated than the zirconia phase. These results are consistent with an earlier study on the composite by Wakai and Kato [19]. The maximum phase elongations recorded in the present study were $\bar{L}_1/\bar{L}_2 = 1.16$ and 1.35 for the zirconia and alumina phase, respectively. However, it is important to note that the observed grain elongations are substantially smaller than those calculated based on individual grains maintaining their volumes, but elongating to the same extent as the tensile specimens. Furthermore, measurements on the composite indicated that the grain aspect ratio remains small even after an elongation of 525% [30].

4.2. Critical evaluation of possible deformation mechanisms

There are several possible theoretical models that are discussed below to identify the dominant deformation

process: these include dislocation creep, diffusion creep and grain-boundary sliding.

4.2.1. Dislocation creep

In general, creep deformation with stress exponents of > 3 are usually attributed to some form of intragranular dislocation motion [31]. It is necessary to consider the stresses necessary to activate dislocation glide on suitable slip systems in order to evaluate the viability of this process. There are no experimental data on flow stresses for slip in tetragonal zirconia, but such data are available for cubic zirconia [27, 28, 32] and alumina [33].

Dominguez–Rodriguez et al. [32] determined experimentally that stresses greater than 150 MPa were necessary to activate slip in yttria-stabilized cubic zirconia tested at 1673 K and a strain rate of $\sim 10^{-5}$ s^{-1}: the flow stresses increased with the Y_2O_3 content in the range 9.4–18 mol %. Inspection of the creep data obtained in the present study, at 1665 K, indicates that a stress of ~ 30 MPa is adequate to obtain a strain rate of $\sim 10^{-5}$ s^{-1}, thereby suggesting that dislocation creep is unlikely in the zirconia phase.

Heuer et al. [33] have compiled data on alumina for the flow stresses necessary for slip on the basal, prismatic and pyramidal systems as a function of temperature. An examination of the data suggests that stresses greater than ~ 50 MPa are necessary for basal slip at a temperature of 1673 K and a strain rate of 4 $\times 10^{-5}$ s^{-1}. The results shown in Fig. 3 indicate that deformation occurs at ~ 50 MPa for a strain rate of 4 $\times 10^{-5}$ s^{-1}. This comparison indicates that some favourably oriented alumina grains may undergo slip, and this limited slip may account for the slightly greater tendency of the alumina phase to elongate along the tensile axis, compared to the zirconia phase. It is important to note that the presence of zirconia as a solute in alumina may increase the stresses necessary for intergranular slip.

It should be noted also that intragranular dislocation creep processes are usually independent of the grain size, $p = 0$ [31]. The observed strong grain-size dependence for creep in the composite, $p = 2$, also suggests that dislocation creep is not the rate-controlling deformation mechanism.

4.2.2. Diffusion creep

In the absence of intragranular dislocation creep, deformation may be attributed to some form of diffusion creep, which occurs solely by the diffusion of vacancies from grain boundaries experiencing tension to those in compression. Depending on whether the vacancy diffusion path is through the matrix or along grain boundaries, the process is referred to as Nabarro–Herring [34, 35] or Coble [36] creep, respectively. Both of these mechanisms predict $n = 1$ and grain elongation along the tensile axis to the same extent as the specimen elongation. Clearly, the observed value of $n \sim 3$ together with the lack of significant grain elongation indicates that the present data cannot be attributed directly to diffusion creep.

4.2.3. Interface reaction-controlled diffusion creep

The classical models for diffusion creep were developed with the implicit assumption that grain boundaries act as perfect sources and sinks for vacancies. However, the process actually involves the creation, transport and annihilation of vacancies: these three steps operate sequentially, so that the slowest one is rate-controlling. When grain boundaries do not act as perfect sources or sinks, the creation or annihilation of vacancies may become the rate-controlling step: creep under such conditions is referred to as interface reaction-controlled diffusion creep.

In general, the standard diffusion creep rate is proportional to the chemical potential difference $(\Delta\mu)$ between boundaries experiencing tensile and compressive stresses: $\Delta\mu \propto \sigma\Omega$, where Ω is the atomic volume. As noted originally by Ashby [37], when grain boundaries do not act perfectly, it is possible to modify the chemical potential difference as $(\Delta\mu-\Delta\mu_i)$, where $\Delta\mu_i$ is the potential difference necessary to drive the interface reaction by emitting or absorbing a vacancy. Two simple possibilities arise from this modification: (i) the diffusion creep rate is reduced, but the process remains Newtonian viscous $(n = 1)$, when $\Delta\mu_i \propto \sigma$, and (ii) the diffusion creep rate is reduced, and diffusion creep ceases to operate below a threshold stress when $\Delta\mu_i$ is a constant. The present experimental creep data exhibit a stress exponent $n \sim 3$, thereby indicating that a process involving $\Delta\mu_i \propto \sigma$ cannot rationalize the creep behaviour of the zirconia–alumina composite. For the alternative explanation described above, $\Delta\mu_i = $ constant, the experimental data should fall on a straight line when the results are plotted as $\dot{\varepsilon}$ versus σ on a linear scale; however, the present experimental results do not follow this behaviour. Furthermore, it is anticipated that the grains would be elongated along the tensile axis because the physical process involved in an interface reaction-controlled process is similar to that in diffusion creep; this is in contrast to the observation that the microstructure remains equiaxed after substantial deformation. Therefore, tensile creep in the composite cannot be attributed to a simple form of an interface reaction-controlled diffusion process.

4.2.4. Grain-boundary sliding and grain rearrangement

The lack of significant grain growth and grain elongation suggests strongly that grain-boundary sliding plays a dominant role in the deformation of the superplastic zirconia–20% alumina composite.

It is important to distinguish between two different types of sliding processes that may occur during high-temperature deformation, as noted originally by Cannon [38]: Lifshitz sliding that occurs naturally as part of diffusion creep, to maintain grain contiguity, and Rachinger sliding which occurs as an independent deformation mechanism. In Lifshitz sliding, the total number of grains on the specimen surface does not change, and the grains elongate along the tensile axis. In contrast, grains remain equiaxed during Rachinger

sliding (grains may elongate along the tensile axis when Rachinger sliding occurs concomitantly with intragranular dislocation creep), so that there is an increase in the number of grains on the tensile surface as the specimen deforms. It is clear from the observation of the maintenance of an equiaxed microstructure that Rachinger sliding is an appropriate process for the present creep study.

Grain-boundary sliding has been widely recognized as a dominant deformation process in superplastic metallic alloys [39, 40]. Gifkins [41] and Langdon [42, 43] have developed physically realistic qualitative three-dimensional models that allow grain rearrangement processes to operate by enabling the emergence of new grains on the tensile surface of superplastically deformed specimens. The present microstructural observations of a lack of any intragranular dislocation activity and the maintenance of an equiaxed microstructure is consistent with this model; however, the qualitative nature of the model precludes a detailed quantitative comparison.

5. Conclusion

This paper provides a first detailed report on the constant stress tensile creep characteristics of a superplastic ceramic. Constant stress tensile creep experiments were conducted over a wide range of experimental conditions on a superplastic 3 mol % yttria stabilized zirconia–20 wt % alumina composite. Creep deformation was characterized by an extensive primary region extending to strains of $\sim 10\%$, over which the strain rate is decreasing, and this was followed by a reasonably well-defined steady-state region. The power law creep behaviour of the composite may be expressed in the form $\dot{\varepsilon} \propto \sigma^n \bar{L}^{-p}\exp(-Q/RT)$, where $\dot{\varepsilon}$ is the steady state creep rate, σ is the imposed tensile stress, $\bar{L}$ is the mean linear intercept grain size, R is the gas constant, T is the absolute temperature, the stress exponent $n = 2.8$, the inverse grain size exponent $p = 2$ and the activation energy $Q = 585$ kJ mol^{-1}. Microstructural observation indicated that there was very little grain growth or grain elongation during creep deformation, and there was no evidence for any intragranular dislocation activity. Based on a detailed analysis of possible mechanisms, it was concluded that creep occurred by a grain-boundary sliding/grain rearrangement process.

References

1. C. E. PEARSON, *J. Inst. Metals.* **54** (1934) 111.
2. R. H. JOHNSON, *Metall. Rev.* **15** (1970) 115.
3. K. A. PADMANABHAN and G. J. DAVIES, "Superplasticity" (Springer, New York, 1980).
4. A. K. MUKHERJEE, T. R. BIELER and A. H. CHOKSHI, in "Materials Architecture", edited by J. B. Bilde-Sorensen, N.

Hansen, D. Juul Jensen, T. Leffers, H. Lilholt and O. B. Pedersen (Riso National Laboratory, Roskilde, Denmark, 1989) p. 207.

5. A. H. CHOKSHI, A. K. MUKHERJEE and T. G. LANGDON, *Mater. Sci. Eng.* **R10** (1993) 237.
6. F. WAKAI, S. SAKAGUCHI and Y. MATSUNO, *Adv. Ceram. Mater.* **1** (1986) 259.
7. T. G. NIEH, C. M. McNALLY and J. WADSWORTH, *Scripta Metall.* **22** (1988) 1297.
8. C. CARRY, in "Superplasticity", edited by M. Kobayashi and F. Wakai (Materials Research Society, Pittsburgh, PA, 1989) p. 199.
9. Y.-I. YOSHIZAWA and T. SAKUMA, *J. Am. Ceram. Soc.* **73** (1990) 3069.
10. Y. OKAMOTO, J. IEUJI, Y. YAMADA, K. HAYASHI and T. NISHIKAWA, in "Science and Technology of Zirconia III", edited by S. Somiya, N. Yamamoto and H. Yanagida (The American Ceramic Society, Columbus, OH, 1988) p. 565.
11. M. NAUER and C. CARRY, *Scripta Metall. Mater.* **24** (1990) 1459.
12. F. WAKAI and T. NAGANO, *J. Mater. Sci. Lett.* **7** (1988) 607.
13. D. M. OWEN and A. H. CHOKSHI, in "Superplasticity in Advanced Materials", edited by S. Hori, M. Tokizane and N. Furushiro (The Japan Society for Research on Superplasticity, Osaka, 1991) p. 215.
14. N. G. PACE, G. A. SAUNDERS, Z. SUMENGEN and J. S. THORP, *J. Mater. Sci.* **4** (1969) 1106.
15. D. H. CHUNG and G. SIMMONS, *J. Appl. Phys.* **39** (1969) 5316.
16. A. H. CHOKSHI, *Mater. Sci. Eng.*, **A166** (1993) 119.
17. D. M. OWEN and A. H. CHOKSHI, *Scripta Metall. Mater.* **29** (1993) 869.
    AYAMA, *Yogyo-Kyokai-Shi* **94** (1986) 1017.
19. F. WAKAI and H. KATO, *Adv. Ceram. Mater.* **3** (1988) 71.
20. T. G. NIEH, C. M. McNALLY and J. WADSWORTH, *Scripta Metall.* **23** (1989) 457.
21. T. G. NIEH and J. WADSWORTH, *J. Mater. Res.* **5** (1990) 2613.
22. D. M. OWEN and A. H. CHOKSHI, in "Science and Technology of Zirconia: Proceedings of Zironia V", edited by S. P. S. Badwal, M. J. Bannister amd R. H. J. Hanmik (Technomic Publishing, Lancester, PA, 1993) p. 432.
23. F. WAKAI, T. IGA and T. NAGANO, *Nippon Serammikkus Kyokai Gakujusu Ronbunshi* **96** (1988) 1206.
24. I.-W. CHEN and L. A. XUE, *J. Am. Ceram. Soc.* **73** (1990) 2585.
25. T. G. NIEH and J. WADSWORTH, *Acta Metall. Mater.* **39** (1991) 3037.

26. W. R. CANNON and T. G. LANGDON, *J. Mater. Sci.* **18** (1983) 1.
27. A. DOMINGUEZ-RODRIGUEZ, A. H. HEUER and J. CASTAING, in "Radiation Effects and Defects in Solids", (Gordon and Breach, UK, 1991) p. 759.
28. J. MARTINEZ-FERNANDEZ, M. JIMENEZ-MELANDO, A. DOMINGUEZ-RODRIGUEZ and A. H. HEUER, in "Euro-Ceramics", edited by G. de With, R. A. Terpstra and R. Metselaar, Vol. 3 (Elsevier Applied Science, London, 1989) p. 318.
29. T. G. NIEH, C. M. TOMASELLO and J. WADSWORTH, in "Superplasticity in Metals, Ceramics, and Intermetallics", edited by M. J. Mayo, M. Kobayashi and J. Wadsworth (Materials Research Society, Pittsburgh, PA, 1990) p. 343.
30. A. H. CHOKSHI, D. J. SCHISSLER, T.-G. NIEH and J. WADSWORTH, in "Superplasticity in Metals, Ceramics, and Intermetallics", edited by M. J. Mayo, M. Kobayashi and J. Wadsworth (Materials Research Society, Pittsburgh, PA, 1990) p. 379.
31. A. H. CHOKSHI and T. G. LANGDON, *Mater. Sci. Tecnol.* **7** (1991) 577.
32. A. DOMINGUEZ-RODRIGUEZ, K. P. D. LAGERLOF and A. H. HEUER, *J. Am. Ceram. Soc.* **69** (1986) 281.
33. A. H. HEUER, N. J. TIGHE and R. M. CANNON, *ibid.* **63** (1980) 53.
34. F. R. N. NABARRO, in "Report of a Conference on Strength of Solids", (The Physical Society, London, 1948) p. 75.
35. C. HERRING, *J. Appl. Phys.* **21** (1950) 437.
36. R. L. COBLE, *ibid.* **34** (1963) 1679.
37. M. F. ASHBY, *Scripta Metall.* **3** (1969) 837.
38. W. R. CANNON, *Philos. Mag.* **25** (1972) 1489.
39. Z.-R. LIN, A. H. CHOKSHI and T. G. LANGDON, *J. Mater. Sci.* **23** (1988) 2712.
40. A. H. CHOKSHI and A. K. MUKHERJEE, in "The Brittle-Ductile Transition in Rocks, Geophysical Monograph 56", edited by A. G. Duba, W. B. Durham, J. W. Handin and H. F. Wang (American Geophysical Union, Washington, DC, 1990) p. 83.
41. R. C. GIFKINS, *J. Mater. Sci.* **13** (1978) 1926.
42. T. G. LANGDON, *Metals Forum* **4** (1981) 14.
43. *Idem, Mater. Sci. Eng.* **A137** (1991) 1.